

Influence of the degree of utilization on the structural behaviour of stainless steel frames subject to fire

Guillermo Segura, Asal Pournaghshband¹, Sheida Afshan¹, Enrique Mirambell²

Correspondence

Guillermo Segura Valdivieso
Universitat Politècnica de Catalunya
Jordi Girona 1-3, Building C1, Room 207
08034 Barcelona, Spain
Email: gseguravaldivieso@gmail.com

Abstract

Stainless steel is known to have a better behaviour at elevated temperatures than carbon steel. This, combined with its aesthetic appeal and corrosion resistance, makes stainless steel structures an attractive alternative to carbon steel structures. However, EN 1993-1-4 does not establish design rules associated with global analysis of stainless steel frames and EN 1993-1-2, devoted to carbon steel, provides a conservative approach for the fire design of stainless steel structures. Hence, current European codes do not provide efficient design guidelines for stainless steel frames subject to fire and therefore the response of this type of structures should be assessed by means of experimental tests and/or numerical analyses.

The main objective of the paper is to assess the nonlinear structural response of stainless steel frames subjected to fire, focusing the investigation on the influence of the degree of utilization. A comprehensive numerical analysis on Class 1 and Class 3 stainless steel frames and Class 1 carbon steel frame subjected to fire is carried out varying the degree of utilization. Calibration of the FE models has been carried out as a part of a study of transient thermo-mechanical models, which are needed to assess the response of stainless steel frames subjected to fire.

Keywords

Stainless steel frames, fire design, thermo-mechanical model, global analysis, degree of utilization

1 Introduction

The corrosion resistance and durability of stainless steel are well known, offering the potential for more sustainable construction with increased structural design lives. Adequate performance of stainless steel structures in fire is however the major obstacle which potentially limits their use in construction, as they are often left without fire protection. While the use of fire protection for stainless steel structures destroys all the reasons for using stainless steel in the first place, i.e. intrinsic durability and aesthetic appeal particularly, other means of providing fire resistance, e.g. through performance based design approach, is needed. While recent years have seen an increase in the research carried out on the structural behaviour and design of stainless steel structural members e.g. beams and columns at elevated temperatures e.g. [1-2], research on stainless steel frame structures in fire has been relatively limited. Following on from the realization of the many benefits of design based on whole frame behaviour in fire of carbon steel structures and building on the existing body of knowledge on fire performance

of stainless steel structures at member level, the current study aims to investigate the global structural behaviour of stainless steel frames in fire. The full load-deformation history of two-dimensional stainless steel frames at elevated temperature is investigated through a comprehensive numerical modelling investigation.

2 Numerical model

Carbon and stainless steel are known to lose their mechanical properties at elevated temperatures, therefore the response of carbon and stainless steel frames subject to fire is directly affected by the temperature field. In order to correctly reproduce the response of steel frames subjected to fire in numerical models, two different analyses need to be conducted: a heat transfer analysis and a mechanical analysis.

Since there is no published data of stainless steel frames tested under fire situation, nine carbon steel frames tested by Rubert and Schaumann [3] were reproduced to validate the finite element model. Based on this validation, an extensive parametric analysis on the effect of the degree of utilization on the response of stainless steel frames subject to fire has been performed.

1. University of Southampton, Southampton, UK.
2. Universitat Politècnica de Catalunya, Barcelona, Spain.

2.1 Description of the numerical model

As stated before, two different numerical analyses must be performed in order to assess the response of carbon and stainless steel frames under fire situation. The FE analysis package ABAQUS [4] was used to develop the sequentially coupled thermo-mechanical model. First, a heat transfer analysis was carried out, obtaining the development over time of the frame temperature field. Afterwards, a mechanical analysis was performed where an initial load is applied at room temperature (20°C), which is maintain constant while the temperature field obtained from the thermal analysis is applied at each time increment.

The heat transfer analysis was performed with a *HEAT TRANSFER step in ABAQUS which is ruled by three physical phenomena: radiation, convection and conduction. Radiation is ruled by the Stefan-Boltzmann constant and the emissivity of the material, which for carbon steel is $\epsilon=0.7$ and for stainless steel is $\epsilon=0.4$ according to the EN 1993-1-2 [5], while emissivity of air is equal to the unit. The convective heat transfer is ruled by the convection coefficient $\alpha_c=25W/m^2K$ as stated in the EN 1993-1-2 [5]. Convection heat transfer is the main source of temperature increase at early fire stages, whereas radiation starts playing as a main role of heat transfer at elevated temperatures. Both heat transfer mechanisms depend on the air furnace temperature, which was defined in the study by the standard ISO 834 [5] fire curve. There are other material properties that rule the whole heat transfer such as specific heat, thermal conductivity and thermal elongation that are temperature dependant, and their values are provided in the EN 1993-1-2 [5].

The mechanical analysis was modelled by two *STATIC steps. In the first step an initial load, equivalent to a certain degree of utilization, is applied, while in the second step the load is maintained constant and the temperature field of the frame starts to increase using the temperature field development obtained by means of the thermal model. In this second step the material properties of the steel decrease as the temperature increase until the frame collapse. All stress-strain relationships used for this study have been obtained using the formulation presented in the EN 1993-1-2 [5], Figure 1 highlights the different strength, f_p and f_y , and stiffness, E , reduction factors for carbon steel compared to the reduction factors of stainless steel at elevated temperatures according to the EN 1993-1-2 [5].

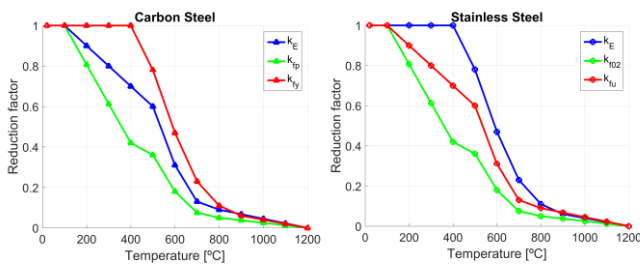


Figure 1 Reduction factors for carbon and stainless steel according to the EN 1993-1-2 [5].

True stress σ_{true} and logarithmic plastic strain ϵ_{ln}^{pl} were implemented in all models, in accordance with the specification of Abaqus [4]. The true stress-strain curve was calculated with equations (1) and (2), from the engineering stress-strain obtained from the codes.

$$\sigma_{true} = \sigma_{nom}(1 + \epsilon_{nom}) \quad (1)$$

$$\epsilon_{ln}^{pl} = \ln(1 + \epsilon_{nom}) - \sigma_{true}/E \quad (2)$$

The 4-node DS4 and S4R and 3-node DS3 and S3R shell elements,

from the ABAQUS element library, were used to discretize the structure. A constant mesh of 5mm×5mm was used for the validation models and an adaptive mesh from 5mm to 15mm was used for the parametric analysis, after realising a mesh convergence study in both cases. Residual stresses were not included in the FE model, since their influence diminishes at elevated temperatures [6].

2.2 Validation of the numerical model

Rubert and Schaumann [3] performed 20 fire tests on different carbon steel frames with three different structural configurations. Since the parametric analysis is carried out only on portal frames, for validation purposes only the one bay frames (EGR) tested in the original paper have been reproduced. All tested frames had pinned supports and their main parameters are presented in Table 1. The geometry of the tested frames is shown in Figure 2.

Table 1 Main parameters of the frames analysed for the parametric study

Frame	L (mm)	h (mm)	F ₁ (kN)	F ₂ (kN)	μ_0	θ (°C)	f _y (MPa)
EGR1b	122	117	65	2.5	0.55	533	382
EGR1c	122	117	65	2.5	0.55	515	382
EGR2	122	117	40	1.6	0.34	612	385
EGR3	122	117	77	3.0	0.66	388	385
EGR4	122	117	77	3.0	0.63	424	412
EGR5	122	117	88	3.4	0.72	335	412
EGR6	122	117	88	3.4	0.72	350	412

All the analysed frames were heated up uniformly. Two vertical loads, F_1 , were applied over the frame columns simultaneously with a horizontal load, F_2 , applied on the right joint. These loads were equivalent to certain degree of utilization μ_0 and were kept constant through the furnace stage (see Table 1). The ultimate load at room temperature was determined by the original authors by means of a second order analysis taking into consideration plastic regions and geometric nonlinearities. The critical temperature θ was defined by the original author as the temperature at which the mid-span deflection reached a value of $L/60$, L being the span length and h being the height of the frame. The lateral torsional buckling of the frame members was prevented by means of various lateral restraints, marked in Figure 2 with crosses.

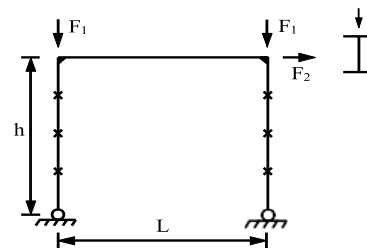


Figure 2 Schematic representation of the tested frames [3]

The measured maximum element imperfection was reported to be $h/3000$ and $L/3000$ and the global frame imperfection was $h/600$. The global imperfection was considered to be small enough to have any effect on the response of the frame, therefore only the geometric imperfections of each element were included in the FE models. The joints between the beam and each column were reported to be perfectly rigid. This was implemented in the FE models by means of column with a very high stiffness in all six degrees of freedom. All frame cross-sections were IPE 80 of carbon steel St37 grade. Using the measured yield stress at room temperature reported by Rubert

and Schaumann [3] and applying the formulation provided by the EN 1993-1-2 [5] the stress-strain relationship at room temperature and at elevated temperatures were obtained (see Figure 3), which were implemented in the FE models.

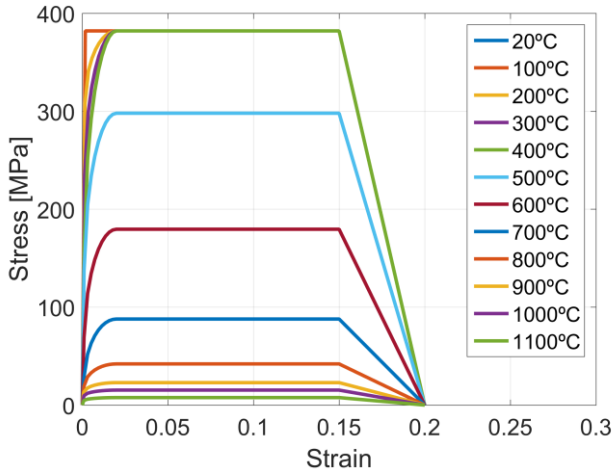


Figure 3 Nominal stress-strain relationship implemented on the FE model for the EGR1b and the EGR1c frame.

The critical temperatures derived from the numerical models were obtained under the same condition of vertical deflection $L/60$ and are presented in table 2. As it can be seen, the mean ratio is 1.036 and the COV is 0.058.

Table 2 Main results of the validation models

Frame	θ_{test} (°C)	θ_{FE} (°C)	$\theta_{test}/\theta_{FE}$
EGR1b	533	509	0.96
EGR1c	515	509	0.99
EGR2	612	600	0.98
EGR3	388	425	1.10
EGR4	424	445	1.05
EGR5	335	371	1.11
EGR6	350	371	1.06
		Mean	1.036
		COV	0.058

Besides the presented validation of the FE model, other validations on cold-formed hollow stainless steel sections at elevated temperatures were performed for previous studies [7]. The accuracy shown by the developed FE models can be considered good enough to perform a parametric analysis on stainless steel frames subject to fire with high reliability.

3 Parametric study

In the following section the influence of the degree of utilization on the response of Class 1 and Class 3 hot-rolled 1.4301 austenitic stainless steel frames is studied. Its structural response is compared to the response of Class 1 S235 hot-rolled carbon steel frames. Both stress-strain relationships were obtained from the EN 1993-1-2 formulation [5].

3.1 Description of the parametric study

In order to properly compare the response of different frames under fire, three different 4x6 frames were designed under the same load combination. The load combination and the frame cross-section were designed according to the EN 1993-1-1 [8] and EN 1993-1-4 [9]. By doing this, all designed frames could have been designed in a real project for a one height building, and therefore it can be highlighted which one would have a better response under fire situation. The main parameters of each frame are presented in Table 3 and in Figure 4.

Table 3 Main parameters of the frames analysed for the parametric study

Parameter	C1 S235	C1 1.4301	C3 1.4301
h (m)	4	4	4
L (m)	6	6	6
d (mm)	200	200	350
b (mm)	120	120	120
t (mm)	8	8	5
r (mm)	20	20	12.5
Supports	fixed-fixed	fixed-fixed	fixed-fixed
α_{cr}	23.5	19.7	21.8
p_1 (kN/m)	27.6	31.8	38.6
$P_1 = p_1 \cdot L$ (kN)	165.6	190.8	231.6
$P_2 = P_1/4$ (kN)	41.4	47.7	57.9

L and h are the frame span length and height, respectively, assuming $L=6m$ and $h=4m$ for all the frames analysed in this parametric study. The cross-section is defined by the parameters d , b , t and r which are the cross-section height, cross-section width, cross-section thickness and corner radii. In other words, the designed cross-section for both Class 1 frames is a RHS200x120x8 and for the Class 3 frame is a RHS350x120x5. In all the studied cases the boundary conditions are fixed-fixed and the designed frames are non-sway at room temperature with an $\alpha_{cr} > 15$. P_1 and P_2 are the ultimate loads at room temperature, when both are applied simultaneously with $P_1/P_2=4$.

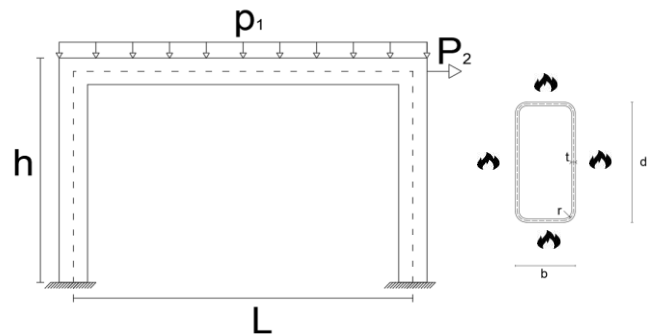


Figure 4 Geometry and loading combination for the analysed frames.

The ratio between the vertical and the horizontal loads is $r = \Sigma F_1/F_2 = 4$ for all studied frames. This ratio was designed for the purpose of triggering the global failure mechanism of the Class 1 frames, see Figure 5. By performing a global rigid plastic analysis, it could be determined that the load ratio needed to be between $r=1.33$ and $r=5.33$ in order to trigger the global failure mechanism rather than the sway mechanism or the beam mechanism. This same mechanism can be seen in Figure 6, which shows the Von Mises stress distribution for the Class 1 carbon steel frame when it is subjected to its ultimate load at 20°C.

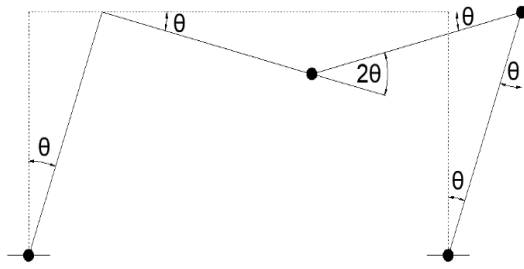


Figure 5 Theoretical global failure mechanism.

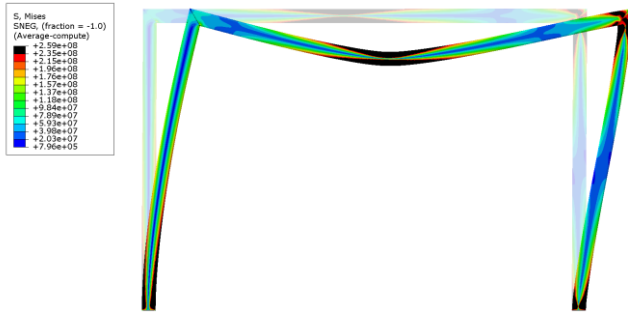


Figure 6 Von Mises stress distribution [N/m²] of the Class 1 carbon steel frame under its ultimate load at room temperature (displacements amplified 5 times).

Once the ratio between the vertical and horizontal load was chosen the ultimate value of P_1 and P_2 was determined by conducting a non-linear mechanical analysis, the ultimate load value was assumed to be the peak of the load-displacement curve of each frame and are presented in Table 3. The vertical load p_1 is uniformly applied onto the beam and do not follow the beam rotation, in the same way the horizontal load P_2 is a point applied onto a reference point constrained to the end cross-section of the beam and do not follow the surface rotation.

For these study cases the joints between the beam and both columns were modelled by means of a steel plate of 16mm (with the same material as the frame). This type of joint does not sufficiently constraint the rotation of the columns and may lead to larger buckling length of the column than expected. The shape of the first sway mode of each frame was included in all models as a geometric imperfection with an amplitude according to the EN 1993-1-1 [8].

The parametric study consists of subjecting the designed frames to fire varying degrees of utilization from $\mu_0=0.2$ to $\mu_0=0.7$ and identifying the effect of this on the critical temperature, the time fire resistance, the vertical and horizontal displacements and if it has any influence on how the frames collapse.

3.2 Numerical convergence issues

When carrying out the parametric study numerical convergence problems appeared in some of the studied cases in the first time increments of the second step, where the temperature started to increase. When this issue appeared, some models could converge in the first time increments and finish the full analysis correctly, whereas other could not converge in these initial time increments, usually below the 15 seconds of the analysis after applying the initial load, and therefore it was not possible to obtain their response to fire.

After some research, this problem was solved modifying the convergence criterion on residuals included in ABAQUS by default. In order to consider that a time increment converged, two error residuals cri-

terion need to be verified. One criterion verifies that the largest residual is less than a certain tolerance R_n^α , whereas the other criterion verifies if the ratio between the largest correction to the largest incremental solution value is less than a certain tolerance C_n^α [3]. It should be noted that in the first time increments of the second step of the problem, where the temperature starts to increase, there is no stress increment, therefore, even a tiny residual may not fulfil the second convergence criterion. ABAQUS Documentation [4] remarks that this second criterion may not be required in some type analyses and can be skipped.

After assessing if removing this criterion had any effect on the final response of the already converged models, this criterion was not checked in the FE models, as some authors had already recommended by Boulbes [10].

4 Results

4.1 Temperature development

In order to obtain the development of the temperature field for the three frames studied a heat transfer analysis was carried out. Their thermal response depends on the material properties and the cross-section geometry, considering the section factor S_m as stated in current codes [5].

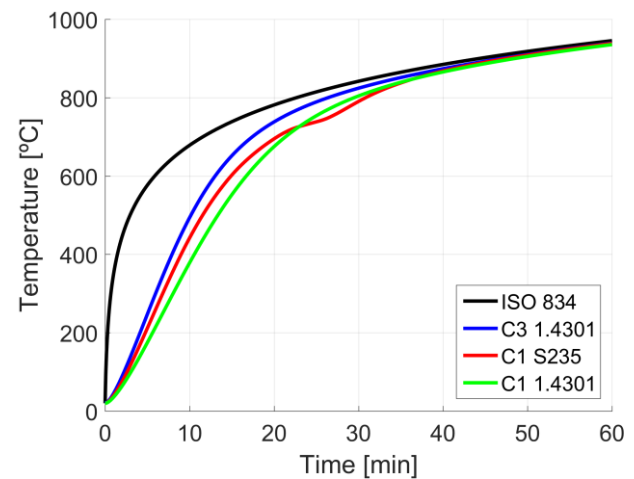


Figure 7 Temperature development over time of the three frames analysed.

Figure 7 shows the thermal response of the three frames studied when they are subjected to fire. The Class 3 stainless steel frame gain temperature faster compared to the Class 1 frames due to its thinner cross-section. A comparison between the temperature results of Class 1 carbon steel frame and Class 1 stainless steel frame allows to conclude that in early stages of fire the temperature increase for the carbon steel is faster than the temperature increase for the stainless steel frame, mainly due to the higher emissivity of the carbon steel. However, when the carbon steel exhibits phase change from 750°C to 780°C, the specific heat increases very abruptly, thereby making that both frames have a similar temperature henceforth.

4.2 Mechanical response under fire

A first approach to understand the different response under fire of each of the designed frames is to compare the exhibit displacements by each one of them before collapsing. Figure 8 shows the representative deformed shape of the frames studied when are subjected to fire and states from which cross-sections of the frame have been obtained the vertical (VD) and horizontal displacements (HD) for the further results analysis.

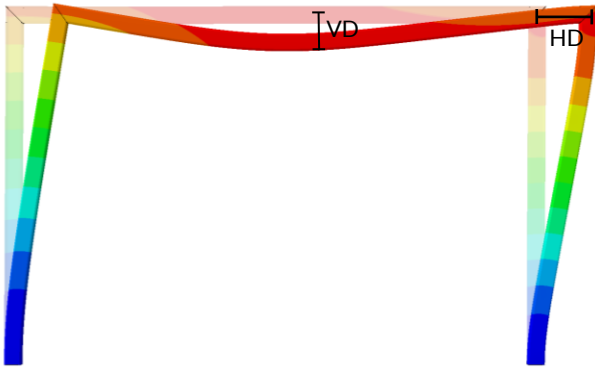


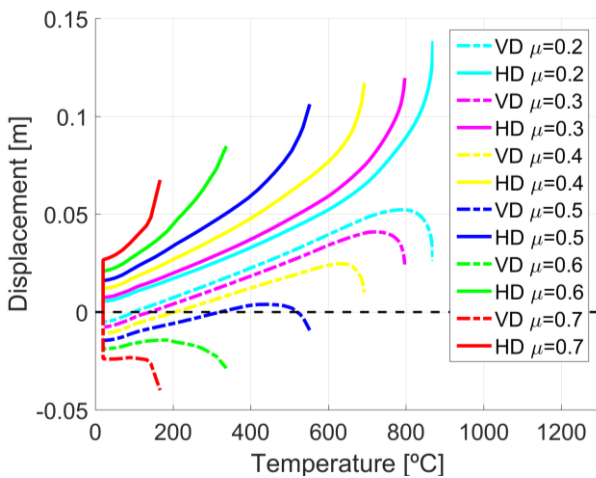
Figure 8 Representative deformed shape of the analysed frames under fire.

Table 4 shows the vertical (VD) and horizontal (HD) displacements of all analysed frames under their critical temperature. Both Class 1 carbon and stainless steel frames exhibit larger displacements than the Class 3 stainless steel frame for all degrees of utilization.

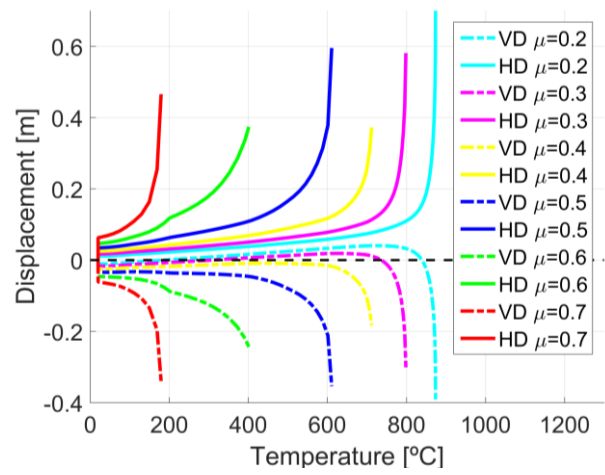
Table 4 Vertical (VD) and horizontal displacements (HD) of the analysed frames under their critical temperature.

	C3 1.4301		C1 1.4301		C1 S235	
	VD (m)	HD (m)	VD (m)	HD (m)	VD (m)	HD (m)
$\mu=0.2$	0.026	0.139	-0.391	0.708	-0.124	0.243
$\mu=0.3$	0.024	0.120	-0.301	0.581	-0.114	0.220
$\mu=0.4$	0.010	0.117	-0.184	0.373	-0.162	0.281
$\mu=0.5$	-0.009	0.106	-0.354	0.595	-0.119	0.211
$\mu=0.6$	-0.029	0.085	-0.244	0.374	-0.181	0.299
$\mu=0.7$	-0.040	0.067	-0.341	0.466	-0.155	0.253

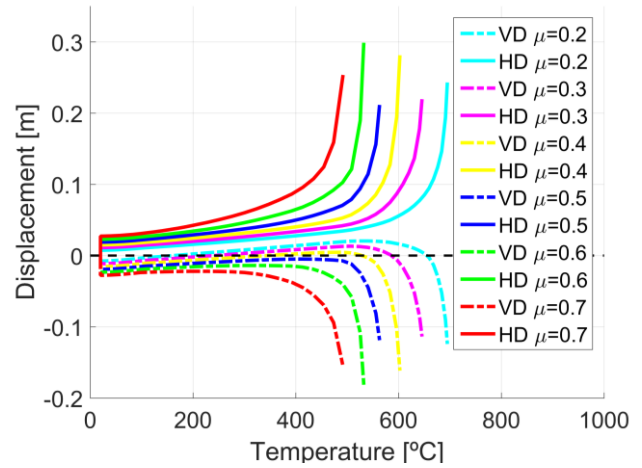
As it has been described in section 3.1 both Class 1 carbon and stainless steel frames were designed in order to form a global failure mechanism at room temperature. The Class 3 stainless steel frame is expected to fail when the critical section reaches the design bending moment resistance. One of the main goals of this study is to assess the influence of the degree of utilization on the type of failure of the frame. Figure 9 shows the horizontal displacement (HD) and vertical displacement (VD) at mid span of the beam of the analysed frames depending on the degree of utilization.



a) Class 3 stainless steel frame



b) Class 1 stainless steel frame



c) Class 1 carbon steel frame

Figure 9 Horizontal displacement (HD) and vertical displacement (VD) at mid span of the beam of the analysed frames.

The three frames exhibit similar response at the first stages of fire, the horizontal displacement (HD) continues to increase with increasing temperatures for all utilisation ratios. The vertical displacement (VD) starts with a downward displacement (indicated as negative on Figure 8) caused by the applied load at room temperature. As the temperature increases, the downward displacement initially reduces due to the thermal elongation of the member. At high temperatures, the rate of increase in the vertical displacement increases as the member stiffness, controlling the mechanical deformation, reduces and the downward mechanical displacements overtakes the thermal expansion of the member, causing final failure.

Table 5 Critical temperature θ_c and fire time resistance t of the analysed frames.

	C3 1.4301		C1 1.4301		C1 S235	
	θ_c (°C)	t (min)	θ_c (°C)	t (min)	θ_c (°C)	t (min)
$\mu=0.2$	869.6	39.0	874.1	41.9	695.1	20.0
$\mu=0.3$	797.0	26.0	798.7	29.4	645.8	17.0
$\mu=0.4$	692.8	17.0	712.1	22.1	602.7	15.0
$\mu=0.5$	552.3	11.6	611.0	17.2	563.2	13.5
$\mu=0.6$	337.4	6.7	401.4	10.6	532.5	12.5
$\mu=0.7$	166.8	3.5	179.4	5.1	492.1	11.3

The critical temperature θ_c was assumed to be the frame temperature of the last converged time increment. In the same way, the time fire resistance is the elapsed time needed to reach that temperature. Based on this failure criterion, the Class 3 stainless steel frame fails when its maximum horizontal deflection is at least $h/100$ (see Figure 9). Assuming the same criterion for both Class 1 carbon and stainless steel frames, a horizontal deflection of about $h/20$ is reached for the stainless steel frames and a horizontal deflection of about $h/30$ is reached for the carbon steel frames for all degrees of utilization studied.

From the results presented in Table 5 and Figure 9 it can be pointed out that for low degrees of utilization ($\mu=0.2$ to $\mu=0.5$), the Class 1 stainless steel frame exhibits a much better performance under fire than the Class 1 carbon steel frame in terms of critical temperature and time fire resistance. Even for the lowest degrees of utilization ($\mu=0.2$ to $\mu=0.4$) the Class 3 stainless steel frame exhibits a better performance under fire than the Class 1 carbon steel frame. However, for higher initial loads ($\mu=0.6$ and 0.7), the Class 1 carbon steel frame has a better response under fire situation than the stainless steel frames. That is due the fact that carbon steel does not lose its yield stress until 400°C , whereas both the yield stress and the ultimate tensile stress of stainless steel start to reduce from 100°C (see Figure 1). As a result, for high degrees of utilization, where the critical temperature is usually lower, the carbon steel frame may perform better under certain fire scenarios.

The Class 3 stainless steel frame has a worse performance in terms of time fire resistance compared with the Class 1 stainless steel frame. Despite having similar critical temperatures, the time fire resistance of the Class 3 stainless steel frames is lower for all degrees of utilization, this is because the Class 3 stainless steel frame gains temperature at a faster rate due to its thinner cross-section (higher section factor S_m) as it is highlighted in Figure 7. In terms of failure mechanism, the analysed Class 3 stainless steel frame collapses when the maximum stress in their critical cross-section (the right beam-column joint) exceeds proof stress $f_{0.2}$ and uses up a fraction of the strain hardening of the material (see Figure 10).

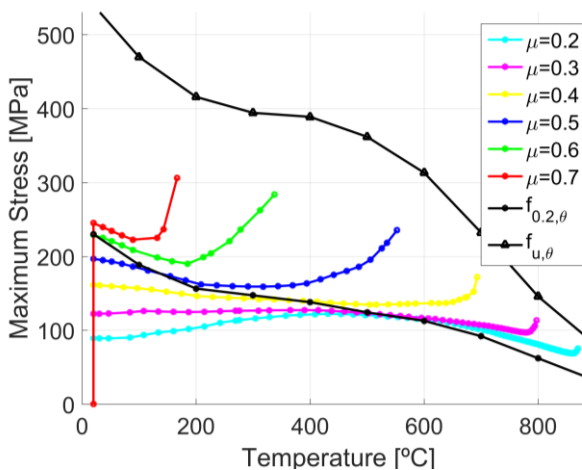
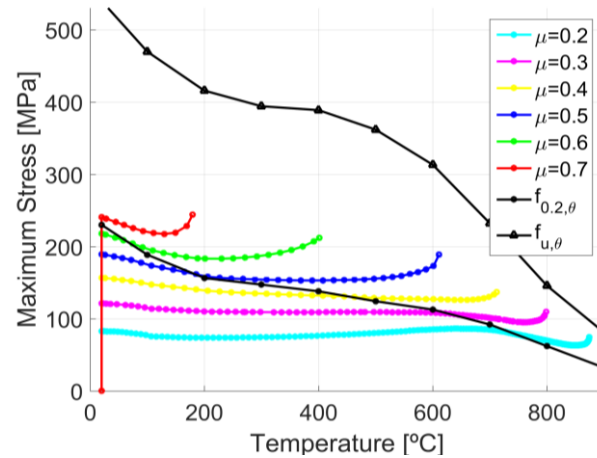


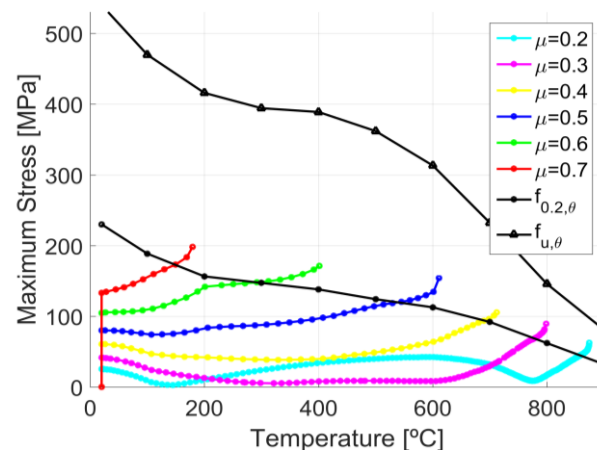
Figure 10 Maximum stress development in the critical cross-section of the Class 3 stainless steel frames (right beam-column joint).

Likewise, Figure 11 shows that the response of the Class 1 stainless steel frame is clearly different because the maximum stress of the critical cross-sections is not reaching the ultimate stress of the material, despite being a Class 1 cross-section, and this occurs for all degrees of utilization studied. Since both Class 1 carbon and stainless steel frames were designed in order to form a global failure mechanism, the collapse of the frames should be governed by the formation of four plastic hinges, involving sway mechanism and

beam mechanism. Figure 11 shows the maximum stress development at the cross-section near the right beam-column joint and at the cross-section close to the left column support.



a) Maximum stress development of the right column-beam joint.



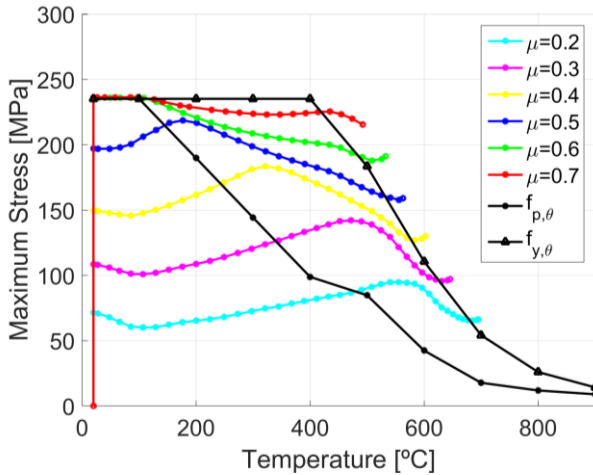
b) Maximum stress development of the left column support.

Figure 11 Maximum stress at the right beam-column joint cross-section a) and at the left column support cross-section b) for the Class 1 stainless steel frames.

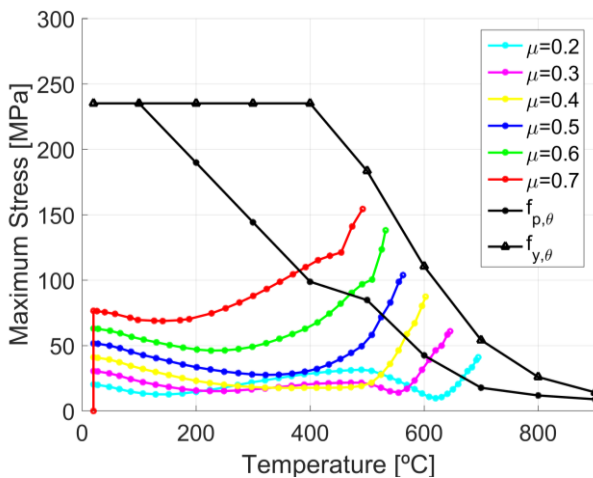
It was observed that the first plastic zone formed in the right beam-column joint and the last one was formed in the left column support. Figure 11 also highlights how the initial applied load produces higher stresses at the right column-beam joint than at the left column support. Then, when the temperature increases, the stress starts to increase first in the right beam-column joint and, when it exceeds the proof stress $f_{0.2}$, the internal forces redistribute and the stress of left column support increases. It can be seen that only for the lowest degrees of utilization ($\mu=0.2$ and $\mu=0.3$) the Class 1 stainless steel frame is using up the inherent strain hardening of stainless steel material. However, as the degree of utilization increases the Class 1 stainless steel frame reaches failure with values of the maximum stress increasingly farther from the ultimate stress of the material. Therefore, it may be concluded that only for the lowest degrees of utilization the Class 1 stainless steel frame is able to form a fully global failure mechanism. This phenomenon can be emphasized when is compared to the stress evolution at the same cross-sections for the Class 1 carbon steel frame (see Figure 12).

Carbon steel does not exhibit strain hardening at elevated temperatures according to EN 1993-1-2 [5] and therefore it reaches its yield stress f_y for lower strain values. As it can be seen in Figure 12, the Class 1 carbon steel frame collapses, for all degrees of utilization considered, when the maximum stress at the critical cross-section,

the right beam-column joint, exceeds the yield stress (the engineering stress-strain curve is used in the FE model).



a) Maximum stress development of the right column-beam joint.



b) Maximum stress development of the left support.

Figure 12 Maximum stress at the right beam-column joint cross-section a) and at the left column support cross-section b) for the Class 1 carbon steel frames.

Afterwards, the internal forces redistribute until the maximum stress at the left column support cross-section is close to the yield stress of the material. For all degrees of utilization considered, the carbon steel frame is forming a global failure mechanism, while the Class 1 stainless steel frame could be considered to form a global failure mechanism only for lowest degrees of utilization.

5 Conclusions

The sequentially coupled thermo-mechanical model is able to reproduce the nonlinear response of steel frames under fire. All analysed frames show great dependency between the degree of utilization, the critical temperature and the time fire resistance. For lower degrees of utilization, both Class 1 and Class 3 austenitic stainless steel frames show better performance under fire than the Class 1 carbon

steel frame, whereas for higher degrees of utilization the carbon steel frame exhibits better fire resistance for the analysed frames.

Moreover, only the Class 1 carbon steel frame is able to form a full global failure mechanism for all degrees of utilization studied, because the Class 1 stainless steel frame does not use up all the material strain hardening before failure. Furthermore, the Class 3 stainless steel frame is able to reach higher stresses at the critical cross-section than the Class 1 stainless steel frame before collapsing.

Acknowledgment

The authors acknowledge the funding from the MINECO (Spain) under Project BIA2016-75678-R, AEI/FEDER, UE "Comportamiento estructural de pórticos de acero inoxidable. Seguridad frente a acciones accidentales de sismo y fuego".

References

- [1] Huang, Y.; Young, B. (2018) *Structural performance of cold-formed lean duplex stainless steel beams at elevated temperatures*. *Thin-Walled Struct.*, 129, pp. 20-27
- [2] Lopes, N.; Vila Real, P.; da Silva, L.; Franssen, J.M. (2010) *Axially loaded stainless steel columns in case of fire*. *Journal of Structural Fire Engineering*, 1 (1), pp 43-60.
- [3] Rubert, A.; Schaumann, P. (1986) *Structural Steel and Plane Frame assemblies under Fire Action*. Essen: Fire Safety Journal, 10, 173-184.
- [4] Abaqus Documentation. Abaqus 2016. Abaqus, Version 6.16. Dassault Systmes, Simulia Corp. USA.
- [5] European Committee for Standardization (CEN) (2005) *EN 1993-1-2:2005. Eurocode 3: Design of Steel Structures – Part 1-2: General Rules. Structural fire design*. Brussels, Belgium.
- [6] Ng, K.T.; Gardner, L. (2007) *Buckling of stainless steel columns and beams in fire*. *Engineering structures* 29(5), 717-730.
- [7] Segura, G.; Afshan, S.; Mirambell, E.; Real, E. (2019) *Numerical analysis of stainless steel frames subject to fire*. *Congress on Numerical Methods in Engineering 2019, CMN19*. Guimaraes, Portugal.
- [8] European Committee for Standardization (CEN) (2005) *EN 1993-1-1. Eurocode 3 – Design of Steel Structures – Part 1-1: General rules and rules for buildings*. Final Document. Brussels, Belgium.
- [9] European Committee for Standardization (CEN) (2006) *EN 1993-1-4:2006. Eurocode 3: Design of Steel Structures – Part 1-4: General Rules. Supplementary Rules for Stainless Steels*. Brussels, Belgium.
- [10] Boulbes, R.J. (2019) *Troubleshooting Finite-Element Modeling with Abaqus: With Application in Structural Engineering Analysis*. Springer. Cham, Switzerland.